

# Addendum to: Edge-Unfolding Nearly Flat Convex Caps

Joseph O’Rourke\*

February 5, 2022

## Abstract

This addendum to [O’R17] establishes that a nearly flat acutely triangulated convex cap in the sense of that paper can be edge-unfolded even if closed to a polyhedron by adding the convex polygonal base under the cap.

## 1 Introduction

The paper [O’R17] established that every sufficiently flat acutely triangulated convex cap has an edge-unfolding to a non-overlapping simple polygon, i.e., a *net*. I used the term “convex cap” in the following sense (where  $\phi(f)$  is the angle the normal to face  $f$  makes with the  $z$ -axis):

Define a *convex cap*  $\mathcal{C}$  of angle  $\Phi$  to be  $C = \mathcal{P} \cap H$  for some  $\mathcal{P}$  and  $H$ , such that  $\phi(f) \leq \Phi$  for all  $f$  in  $\mathcal{C}$ . [...] Note that  $\mathcal{C}$  is not a closed polyhedron; it has no “bottom,” but rather a boundary  $\partial\mathcal{C}$ .

This note proves that same claim holds even when  $\mathcal{C}$  is closed to a polyhedron by adjoining the convex base face  $B$  bounded by  $\partial\mathcal{C}$ . Eventually this addendum will be incorporated into a future version [O’R17]. For now we assume familiarity with that paper, and especially the section below, the most relevant portions of which we reproduce verbatim. Ellisions are marked by “[...]”.

## 2 Angle-Monotone Spanning Forest

[...]

---

\*Department of Computer Science, Smith College, Northampton, MA, USA. [jorourke@smith.edu](mailto:jorourke@smith.edu).

## 2.1 Angle-Monotone Spanning Forest

“It was proved in [LO17] that every nonobtuse triangulation  $G$  of a convex region  $C$  has a boundary-rooted spanning forest  $F$  of  $C$ , with all paths in  $F$   $90^\circ$ -monotone. We describe the proof and simple construction algorithm before detailing the changes necessary for acute triangulations.

Some internal vertex  $q$  of  $G$  is selected, and the plane partitioned into four  $90^\circ$ -quadrants  $Q_0, Q_1, Q_2, Q_3$  by orthogonal lines through  $v$ . Each quadrant is closed along one axis and open on its counterclockwise axis;  $q$  is considered in  $Q_0$  and not in the others, so the quadrants partition the plane. It will simplify matters later if we orient the axes so that no vertex except for  $q$  lies on the axes, which is clearly always possible. Then paths are grown within each quadrant independently, as follows. A path is grown from any vertex  $v \in Q_i$  not yet included in the forest  $F_i$ , stopping when it reaches either a vertex already in  $F_i$ , or  $\partial C$ . These paths never leave  $Q_i$ , and result in a forest  $F_i$  spanning the vertices in  $Q_i$ . No cycle can occur because a path is grown from  $v$  only when  $v$  is not already in  $F_i$ ; so  $v$  becomes a leaf of a tree in  $F_i$ . Then  $F = F_1 \cup F_2 \cup F_3 \cup F_4$ .

We cannot follow this construction exactly in our situation of an acute triangulation  $G$ , because the “quadrants” for  $\theta$ -monotone paths for  $\theta = 90^\circ - \Delta\theta < 90^\circ$  cannot cover the plane exactly: They leave a thin  $4\Delta\theta$  angular gap; call the cone of this aperture  $g$ . We proceed as follows. Identify an internal vertex  $q$  of  $G$  so that it is possible to orient the cone-gap  $g$ , apexed at  $q$ , so that  $g$  contains no internal vertices of  $G$ . See Fig. 1 for an example. Then we proceed just as in [LO17]: paths are grown within each  $Q_i$ , forming four forests  $F_i$ , each composed of  $\theta$ -monotone paths.

It remains to argue that there always is such a  $q$  at which to apex cone-gap  $g$ . Although it is natural to imagine  $q$  as centrally located (as in Fig. 1), it is possible that  $G$  is so dense with vertices that such a central location is not possible. However, it is clear that the vertex  $q$  that is closest to  $\partial C$  will suffice: aim  $g$  along the shortest path from  $q$  to  $\partial C$ . Then  $g$  might include several vertices on  $\partial C$ , but it cannot contain any internal vertices of  $G$ , as they would be closer to  $\partial C$ . Again we could rotate the axes slightly so that no vertex except for  $q$  lies on an axis.”

[...] (End quoted text.)

## 3 Unfolding the Base $B$

By our definition of a convex cap, its boundary  $\partial C$  lies in a plane, and so bounds a convex polygonal base  $B$ . We assume that, unlike the cap  $C$ ,  $B$  is not triangulated, and so must be unfolded as an intact unit. (Of course, it can be unfolded as a unit even if triangulated.)

Let  $C_\perp$  be the unfolded net of  $C$  produced by the algorithm in [O’R17]. If some edge  $e$  of  $C_\perp$  lies on the convex hull of  $C_\perp$ , then  $B$  can be “flipped out” to  $B'$  around  $e$  by cutting all edges of  $\partial C$  except for  $e$ . Because  $B'$  is convex and is attached to the hull of  $C_\perp$ , it is clear there is no overlap, and we

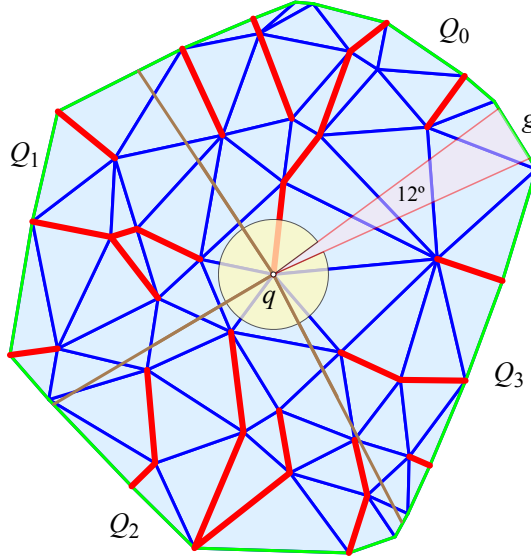


Figure 1: Here the near-quadrants  $Q_i$  have width  $\theta = 87^\circ$ , so the gap  $g$  has angle  $4\Delta\theta = 12^\circ$ .

would be finished. In fact this is the proof path we will follow, but it is not as straightforward as it might seem.

### 3.1 Obstructions

We now argue that there is an arbitrarily flat convex cap  $\mathcal{C}$  and a spanning cut forest  $\mathcal{F}$  such that there is no such edge  $e$  of  $C_\perp$  to which to attach  $B'$  without overlap. First, we look at a “real” unfolding to see what form the obstruction might take. Fig. 2 shows a portion of  $C_\perp$ , identifying a particular edge  $e$  which is tilted inside the hull and would lead to overlap were  $B'$  attached there. However, even in this example, there are many other candidates for  $e$  that would suffice as  $B$ ’s attachment. This suggests the next question: Is there a cap  $\mathcal{C}$  and a cut forest  $\mathcal{F}$  such that every edge of  $C_\perp$  is similarly titled inside the hull, leaving no “safe” attachment edge for  $B$ ? The answer is YES. We only sketch the argument before discussing in more detail how to circumvent this counterexample.

Let  $\mathcal{C}$  be a cap whose boundary  $\partial\mathcal{C}$  is a 12-sided regular polygon (i.e., a dodecagon). For the construction to work, we need at least a 9-sided polygon; 12 makes it visually clearer. The cut forest  $\mathcal{F}$  is as illustrated in Fig. 3: one tree in  $\mathcal{F}$  is a 2-path from the center of  $\mathcal{C}$ , and all the others trees are single segments. The key property is that each segment creates a very shallow angle with  $\partial\mathcal{C}$ .

We arrange near-zero curvature at the central vertex, and all the other vertices have the same curvature  $\omega > 0$ . Because of the shallow angle they form

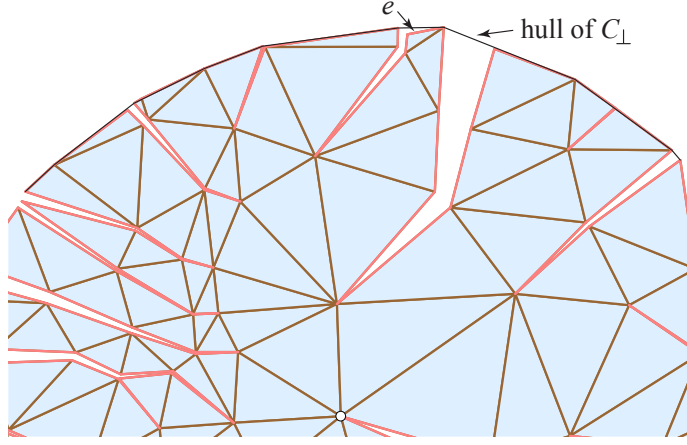


Figure 2: Detail from Fig. 24 of [O'R17], with a portion of the convex hull marked.

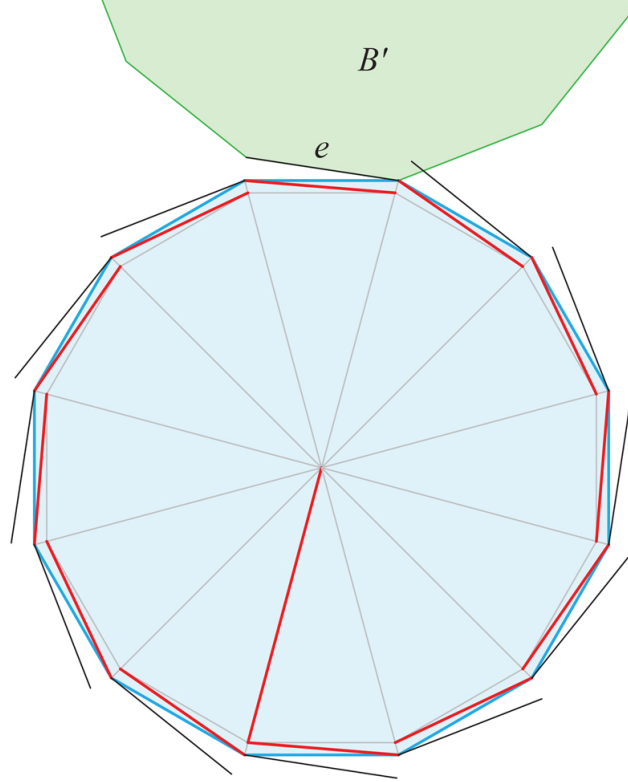


Figure 3: No edge of  $C_\perp$  is a convex hull edge. The cut forest  $F$  is shown red,  $\partial\mathcal{C}$  is blue, developed edges of  $C_\perp$  black.

with  $\partial\mathcal{C}$ , the opening gap caused by cutting each segment is nearly orthogonal to the cut segment. With the internal angle of a 12-gon  $\frac{5}{6}\pi$ , the exterior angle between  $B$  and a reflected copy  $B'$  of  $B$  is  $\frac{2}{6}\pi = 60^\circ < 90^\circ$ . This allows the orthogonally jutting rotation of each boundary edge to penetrate into a reflected  $B'$ , reflected about the next edge  $e$  counterclockwise, as illustrated.

There is no impediment to realizing this example in 3D so that the curvatures  $\omega$  suffice to render every boundary edge of  $C_\perp$  leading to overlap with  $B'$ . Moreover, this could be accomplished for an arbitrarily flat  $\mathcal{C}$  by increasing the number of sides of the  $n$ -gon base so that even a very small  $\omega$  results in overlap. These claims will not be justified further, as they only serve to motivate the next steps.

### 3.2 Quadrant-based forest $F$

The reason the preceding counterexample does not present an insurmountable obstacle is that the spanning forest  $F$  selected in the planar projection graph  $G$  of  $\mathcal{C}$  is not arbitrary, but instead is based on the quadrants illustrated in Fig. 1. We now show that the quadrant-based forest  $F$  leads to an edge  $e$  of  $C_\perp$  to which to attach the reflected base  $B'$ .

A reminder on the notation we are employing:  $\mathcal{C}$  is the convex cap in  $\mathbb{R}^3$ ,  $C$  is its projection on the  $xy$ -plane,  $F$  the spanning forest in that plane,  $\mathcal{F}$  the lift of the forest, and  $C_\perp$  is the development of the cap  $\mathcal{C}$  after cutting  $\mathcal{F}$ .

Let  $v \in \partial\mathcal{C}$  be a vertex on the boundary of the projection  $C$  that is a root of a tree in the forest  $F$ . Rather than viewing the lift, cut, and development as producing  $C_\perp$ , it will help to view the movement of  $v$  in the plane caused by opening the curvatures along the cut paths terminating at  $v$ . As we saw in Section 8 of [O'R17], we can view each cut path  $Q$  to  $v$  as two planar polygonal chains  $L$  and  $R$  which are initially identical, and then open at each vertex  $v_i$  along  $Q$  by the curvatures  $\omega_i$ . Here we are only interested in the final planar displacement of the root  $v$ , the endpoint of the chain. Let  $v$  and  $v'$  be the original and displaced versions of  $v$ , i.e., the last vertices of  $L$  and  $R$ . The *gap segment*  $vv'$  represents the gap at the boundary of  $C_\perp$  caused by opening the cuts in  $F$  to  $v$ , visible, for example, in Fig. 2.

The gap segment  $vv'$  is caused by the composition of several (small) rotations about different centers, the vertices along  $Q$ . It is well-known that  $vv'$  is equivalent to a single rotation about a (generally) different center  $c$ , which we'll call the *composite center of rotation*. We claim that, for sufficiently small  $\omega_i$ ,  $c$  is either inside the convex hull of  $Q$ , or arbitrarily close to the boundary of the hull. This claim is justified in the Appendix by Lemma 2.

Returning to Fig. 3, the centers of rotation in  $F$  were arranged so that the gap segments were nearly orthogonal to  $\partial\mathcal{C}$ , so that they “juttied out” and caused overlap with the reflected  $B'$ . We now argue first, that a different arrangement of centers of rotation can produce “safe” gap segments, and second, that this can be achieved by a quadrant-based spanning forest  $F$ .

Arrange an edge  $e = (v, u)$  of  $\partial\mathcal{C}$  to be topmost and horizontal and crossing the vertical quadrant boundary, and suppose both  $v$  and  $u$  are roots of cut trees

in  $F$ . We call  $e$  a *locally safe edge* if the composite centers of rotation  $c_v$  and  $c_u$  for the trees incident to  $v$  and  $u$  fall underneath  $e$ , as illustrated in Fig. 4. For then the gap segments angle down below  $e$ , making  $e$  a safe candidate for the attachment of  $B'$ .

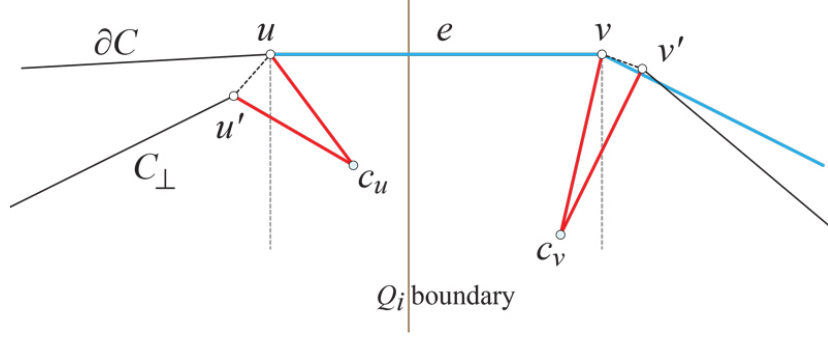


Figure 4: Safe edge  $e$ .

Returning to Fig. 1, we now argue that what was there called the gap edge  $g$  of  $\partial C$  can serve as a safe edge  $e$ . As in that figure, let  $q$  be the quadrants origin. The shortest path  $\gamma$  on  $\mathcal{C}$  to  $\partial C$  is orthogonal to a boundary edge  $e$ . The development of the geodesic  $\gamma$  is a straight line. Use this straight line as the vertical axis of the quadrants, with  $e$  horizontal. Now, because the spanning forest algorithm grows edges within the quadrant wedges, we are guaranteed that all edges of a tree incident to the endpoints of  $e$  are slanted such that they angle strictly vertically underneath  $e$ , as illustrated in Fig. 5. The strictness follows because the wedges are  $\Delta\theta$  less than  $90^\circ$ .

Now applying Lemma 2, we obtain that the composite center of rotation is underneath  $e$ . Even though that lemma allows the true center to be slightly outside the hull of the rotation centers, that the wedges have angle less than  $90^\circ$  permits the conclusion that the true center is in the hull for sufficiently small  $\omega_i$ , and therefore strictly underneath  $e$ . Thus we know that  $e$  is a locally safe edge.

But now it is easy to reapply this argument to conclude that none of the gap segments for other vertices around  $\partial C$  are angled above the horizontal, and so  $e$  is in fact globally safe. Thus we can attach the reflected base  $B'$  along  $e$  without overlap. This proves:

**Theorem 1** *A convex polyhedron consisting of a nearly flat acutely triangulated convex cap  $\mathcal{C}$  joined along  $\partial C$  to a base  $B$  can be edge-unfolded without overlap, for sufficiently small cap curvature  $\Omega$ .*

Using the error between the true and approximate composite rotation centers  $\delta = \frac{1}{2} \sum_i \ell_i \omega_i$  from Lemma 1, and crudely summarizing this as  $\delta = L\omega/2$  for a total chain length  $L$ , a calculation shows the wedge slant  $\Delta\theta$  leads to “sufficiently

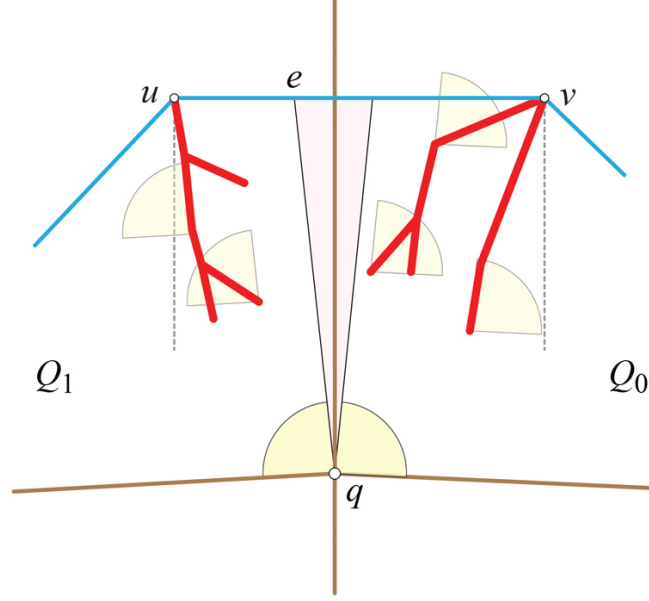


Figure 5: The trees incident to the endpoints of  $e$  have composite centers of rotation underneath  $e$ .

small” curvatures satisfied if  $\omega \lesssim 2\Delta\theta$ . But already we know that

$$\Omega < \pi\Phi^2 < \pi(0.3\sqrt{\Delta\theta})^2 \approx 0.28\Delta\theta ,$$

and because  $\omega < \Omega$  for any one tree of  $F$ , the curvatures are already “sufficiently small” from other constraints.

An illustration is shown in Fig. 6. The selection of  $e$  in this example does not follow the proof exactly just due to limitations of my implementation ( $q$  is not closest to  $\partial\mathcal{C}$  and  $e$  is not orthogonal to the vertical quadrant axis), but it illustrates how  $e$  is locally and indeed globally safe. (In this and in most examples, there are many safe edges.)

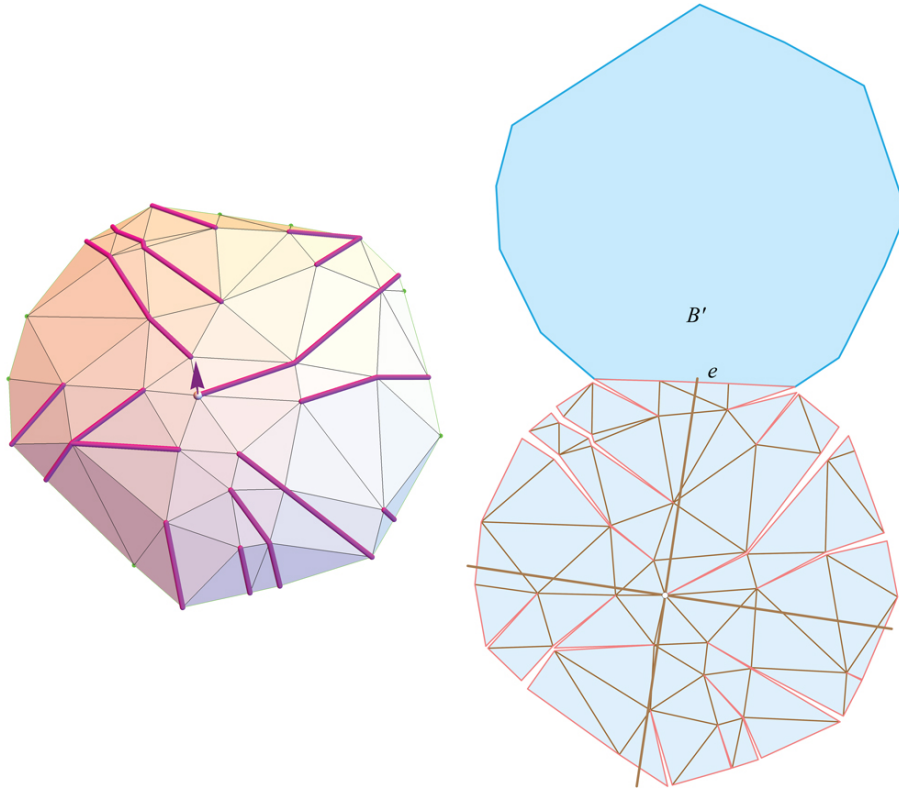


Figure 6: Cap  $\mathcal{C}$  (left) and an edge-unfolding (right), including base  $B$  flipped across safe edge  $e$ .



## Appendix

We need a lemma that allows us to conclude that, for small curvatures, the effect of the rotations along a cut path  $Q$  to a boundary vertex  $v \in \partial C$  is equivalent to one rotation from a point in the convex hull of the vertices along  $Q$ .

**Lemma 1** *Let  $R_i(\omega_i, p_i)$  be a two-dimensional rotation by angle  $\omega_i \geq 0$  about point  $p_i$ , for  $i = 1, \dots, k$ . Then, for sufficiently small  $\omega_i$ , the result of composing the  $k$  rotations  $R_i$  is equivalent to one rotation about a center-of-gravity rotation center: the sum of the  $p_i$  weighted by the angles:*

$$R_1(\varepsilon\omega_1, p_1) \circ \dots \circ R_k(\varepsilon\omega_k, p_k) \rightarrow R(\varepsilon\omega, p)$$

as  $\varepsilon \rightarrow 0$ , where

$$\omega = \sum_i \omega_i$$

and

$$p = (\omega_1 p_1 + \dots + \omega_k p_k) / \omega .$$

The role of  $\varepsilon$  is to ensure all the angles approach 0. Equivalently (and more appropriate in our context), we can just think of the  $\omega_i$  as “sufficiently small.” This proposition is illustrated in Fig. 7 for a polygonal chain.

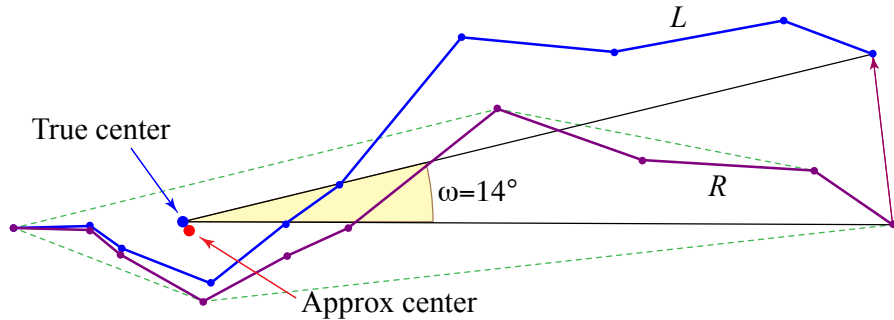


Figure 7: Comparison of true composite center of rotation, and the approximate center-of-gravity center. Here  $R$  is fixed and  $L$  obtained by  $\omega_i$  rotations.

**Proof:** It is well-known that the composition of two rotations by angles  $\omega_1, \omega_2$  about different centers  $p_1, p_2$  is equivalent to one rotation by  $\omega_1 + \omega_2$  about a (generally) different center  $c$ .<sup>1</sup> Consequently, the same holds for the composition of  $k$  rotations. We now prove that as  $\omega_1, \omega_2$  approach 0, the center  $c$  approaches the point  $p = (\omega_1 p_1 + \omega_2 p_2) / (\omega_1 + \omega_2)$  on the  $p_1 p_2$  segment. Following [Nee98, p.38], we view the rotations by  $\omega_1, \omega_2$  as reflections in lines separated

<sup>1</sup> Unless  $\omega_1 + \omega_2 = 2\pi$ , which will never occur with small rotations.

by  $\omega_1/2, \omega_2/2$ . Then  $c$  is the intersection of two reflection lines, as illustrated in Fig. 8. With  $p_1 = (0, 0)$  and  $p_2 = (1, 0)$ , explicit calculation yields

$$c = \left( \frac{\sin \omega_2}{\sin \omega_1 + \sin \omega_2}, \frac{\sin \omega_1 \sin \omega_2}{\sin \omega_1 + \sin \omega_2} \right).$$

From this expression and that for  $p$  above, further calculation shows that the error  $\delta = |c - p|$  is  $\frac{1}{8}(\omega_1 + \omega_2)$  for small  $\omega_i$ . So indeed  $\delta$  approaches zero.

Repeating the argument for  $k$  rotations yields (via a calculation not shown here) that the error  $\delta$  is bounded by  $\frac{1}{2} \sum_i \ell_i \omega_i$ , where  $\ell_i = |p_{i+1} - p_i|$  are the link lengths of the chain, as  $\omega_i \rightarrow 0$ . Thus,  $\delta \rightarrow 0$ ,  $c$  approaches  $p$ , and the claim of the lemma is established.  $\square$

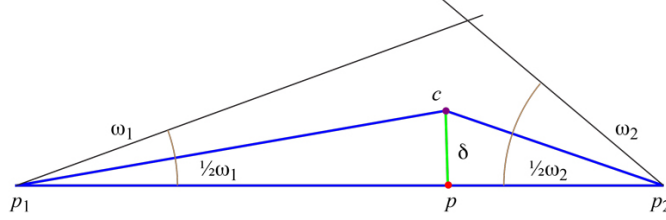


Figure 8: The error  $\delta$  between the true composite center  $c$  and the center-of-gravity center.

An immediate implication of Lemma 1 is:

**Lemma 2** *Under the same assumptions, the center-of-gravity approximate center  $p$  approaches a point in the convex hull of  $\{p_1, \dots, p_k\}$  as  $\varepsilon \rightarrow 0$ , or equivalently, as  $\omega \rightarrow 0$ .*

**Proof:** With  $\omega_i \geq 0$ , the weighted sum in Lemma 1 is a convex combination of the  $p_i$  points, and so inside (or on the boundary of) the convex hull.  $\square$

## References

- [LO17] Anna Lubiw and Joseph O’Rourke. Angle-monotone paths in non-obtuse triangulations. In *Proc. 29th Canad. Conf. Comput. Geom.*, August 2017. arXiv:1707.00219 [cs.CG]: <https://arxiv.org/abs/1707.00219>.
- [Nee98] Tristan Needham. *Visual Complex Analysis*. Oxford University Press, 1998.
- [O’R17] Joseph O’Rourke. Edge-unfolding nearly flat convex caps. arXiv:1707.01006v2 [cs.CG]. <http://arxiv.org/abs/1707.01006>, 2017.